

## Research Article

Theme: Quality by Design: Case Studies and Scientific Foundations

Guest Editors: Robin Bogner, James Drennen, Mansoor Khan, Cynthia Oksanen, and Gintaras Reklaitis

# Investigating Gabapentin Polymorphism Using Solid-State NMR Spectroscopy

Kassibla E. Dempah,<sup>1,2</sup> Dewey H. Barich,<sup>2</sup> Aditya M. Kaushal,<sup>3</sup> Zhixin Zong,<sup>4</sup> Salil D. Desai,<sup>4</sup>  
Raj Suryanarayanan,<sup>3</sup> Lee Kirsch,<sup>4</sup> and Eric J. Munson<sup>1,5,6</sup>

Received 5 June 2012; accepted 21 October 2012; published online 22 November 2012

**Abstract.** Solid-state NMR spectroscopy (SSNMR), coupled with powder X-ray diffraction (PXRD), was used to identify the physical forms of gabapentin in samples prepared by recrystallization, spray drying, dehydration, and milling. Four different crystalline forms of gabapentin were observed: form I, a monohydrate, form II, the most stable at ambient conditions, form III, produced by either recrystallization or milling, and an isomorphous desolvate produced from desolvating the monohydrate. As-received gabapentin (form II) was ball-milled for 45 min in both the presence and absence of hydroxypropylcellulose (HPC). The samples were then stored for 2 days at 50°C under 0% relative humidity and analyzed by <sup>13</sup>C SSNMR and PXRD. High-performance liquid chromatography was run on the samples to determine the amount of degradation product formed before and after storage. The <sup>1</sup>H *T*<sub>1</sub> values measured for the sample varied from 130 s for the as-received unstressed material without HPC to 11 s for the material that had been ball-milled in the presence of HPC. Samples with longer <sup>1</sup>H *T*<sub>1</sub> values were substantially more stable than samples that had shorter *T*<sub>1</sub> values. Samples milled with HPC had detectable form III crystals as well. These results suggest that SSNMR can be used to predict gabapentin stability in formulated products.

**KEY WORDS:** grinding; polymorphism; relaxation time; solid-state NMR; stability.

## INTRODUCTION

Gabapentin, 2-[1-(aminomethyl)cyclohexyl]acetic acid, is used for the treatment of epilepsy and neuropathic pains. Three polymorphic forms of anhydrous gabapentin (forms II, III, and IV) and gabapentin monohydrate (form I) have been reported (1). Thermogravimetric analysis (TGA) of form I revealed a weight loss of ~9%, close to the stoichiometric water content of 10% in the monohydrate (2). Form II, an anhydrous form, is thermodynamically stable under ambient conditions. Form III is metastable while form IV has not been well-characterized. Co-crystals of gabapentin, with numerous carboxylic acid cofomers, have been reported (3,4). A number of studies used Fourier transform infrared spectroscopy (FTIR) to investigate the effect of various processing methods on the polymorphism of gabapentin (2,5).

Gabapentin degrades to a cyclic lactam *via* an intramolecular cyclization reaction triggered by a nucleophilic attack of the hydroxyl group by the nitrogen of the amino group, followed by a dehydration reaction (Scheme 1). This degradation reaction is pH-dependent. The rate of lactamization of gabapentin in lyophilized samples has been studied in the presence of a variety of excipients and at different humidity conditions (6). Recently, Zong and coworkers investigated the effect of milling on both the physical and chemical stability of gabapentin. They milled form II for 15–60 min and stored the samples at 50°C, at relative humidity values ranging from 5% to 80%. The chemical instability, based on the amount of gabapentin lactam formed, was measured by reverse phase high-performance liquid chromatography (HPLC) (7). While milling did not cause any physical transformation, the amount of lactam formed increased with milling time. Moisture had an unusual stabilizing effect and prevented further degradation to the lactam. They concluded that while milling is known to introduce lattice disorder, moisture may bring about recrystallization (“healing of the crystal defects”) and thereby stabilize the material.

In the investigations reported so far, characterization of the physical form of gabapentin has relied primarily on differential scanning calorimetry (DSC), TGA, powder X-ray diffractometry (PXRD), and FTIR. The PXRD patterns of all the forms of gabapentin are characterized by numerous peaks. When there is a mixture of physical forms, their characterization becomes complicated due to the pronounced overlap of PXRD peaks. This problem is further exacerbated in the presence of

<sup>1</sup> Department of Pharmaceutical Sciences, University of Kentucky, Lexington, Kentucky, USA.

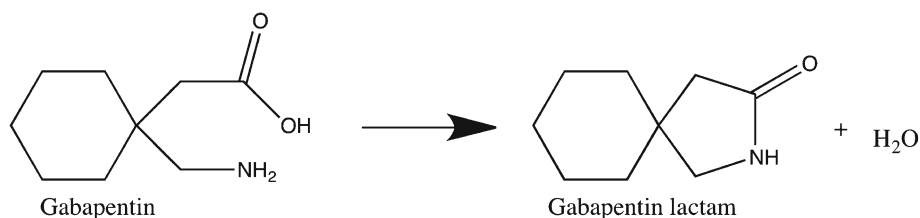
<sup>2</sup> Department of Pharmaceutical Chemistry, University of Kansas, Lawrence, Kansas, USA.

<sup>3</sup> Department of Pharmaceutics, University of Minnesota, Minneapolis, Minnesota, USA.

<sup>4</sup> Division of Pharmaceutics, University of Iowa, Iowa City, Iowa, USA.

<sup>5</sup> 789 S Limestone, Lexington, Kentucky 40536, USA.

<sup>6</sup> To whom correspondence should be addressed. (e-mail: eric.munson@uky.edu)



**Scheme 1.** Degradation of gabapentin

crystalline excipients. Similar difficulties were encountered with the use of FTIR. Similarly, the major limitation of DSC is the overlap of the endothermic melting events of the different forms of gabapentin. In addition, the melting temperatures reported for the polymorphs are not consistent (2,8).

In this paper, we show how solid-state NMR spectroscopy (SSNMR), coupled with PXRD and DSC, can be used to identify the physical form of gabapentin in samples prepared by different methods and in samples milled and subsequently placed under a variety of humidity and temperature conditions. The effect of an excipient, hydroxypropylcellulose (HPC), on the physical and chemical stability of gabapentin was also investigated. SSNMR relaxation times were measured.  $^1\text{H}$  spin lattice relaxation times ( $^1\text{H } T_1$ ) are a well-known indicator of the amount of mobility and of disorder present in a material. We have previously reported that grinding causes a decrease in  $^1\text{H } T_1$  times and stated that “relaxation measurements performed on dosage forms could potentially be used to predict stability of pharmaceutical formulations.” (9) In this study, we show how SSNMR relaxation times were correlated to the propensity of the gabapentin to degrade to the lactam.

The work presented here was part of a multi-institutional project, where gabapentin was used as a model compound. Other research performed in the context of this project includes the work reported by Zong and coworkers (7). Additional reports are expected.

## MATERIALS AND METHODS

Gabapentin (form II) was obtained from Hangzhou Starshine Pharmaceutical Co. LTD (Hangzhou, China). Gabapentin lactam was purchased from Sigma-Aldrich (St. Louis, Missouri). Gabapentin form I was prepared using the method of Ibers by dissolving 160 mg of gabapentin form II in 1 mL of water, adding 3 mL of 2-propanol to it, and keeping it in the freezer for 6 days (10). The isomorphous desolvate mentioned later in the paper was generated during a SSNMR experiment performed on gabapentin form I. Gabapentin form III was crystallized from a saturated 95% ethanol solution at 60°C. That temperature was kept constant throughout the crystallization process.

### Milling

Samples were ground in a planetary mill (Pulviserette 7, Planetary Micro Mill) for 45 min with four hardened steel balls (15 mm).

### Polarized Light Microscopy

Samples were imaged on a polarized light Olympus microscope (Center Valley, PA) under a  $\times 20$  objective.

## Chromatographic Methods

A Thermo Spectrum HPLC System (P4000 pump, AS3000 auto injector, and UV 6000 LP photodiode array detection system) was used to quantify gabapentin and gabapentin lactam. The results are reported as a mole percentage (*w/w*) of total gabapentin (gabapentin + gabapentin lactam). The amount of gabapentin lactam generated during milling was determined from HPLC of samples before and after milling. An aliquot of each of the gabapentin samples was stored at 50°C and 0% relative humidity for 24 h and then subjected to HPLC. This enabled us to quantify the chemical degradation brought about by thermal stress.

## Powder X-ray Diffractometry

The diffraction patterns were collected using a wide angle X-ray diffractometer (model D5005, Bruker, Madison, Wisconsin) at ambient temperature. The instrument was operated in a step-scan mode, in 0.05° 2 $\theta$  steps, and counts were accumulated for 1.0 s at each step over the range of 5 to 40° 2 $\theta$ .

## SSNMR Spectroscopy

$^{13}\text{C}$  SSNMR spectra were collected using either a Chemagnetics CMX300 (Varian, Palo Alto, California), a Bruker Avance 300 (Bruker, Billerica, Massachusetts), or a Tecmag Apollo (Tecmag, Inc., Houston, Texas) spectrometer all operating at a  $^{13}\text{C}$  frequency of ~75 MHz. Each sample was packed under ambient conditions in a 7-mm zirconia rotor (Revolution NMR, Fort Collins, Colorado). 3-Methylglutaric acid was used as an external standard, with methyl peak referenced to 18.84 ppm (11). All spectra were acquired using ramp cross polarization and magic angle spinning (CP/MAS) (12-14). A SPINAL-64 decoupling pulse sequence was used, and the spinning side bands were suppressed using total sideband suppression (15,16). A contact time of 1 ms, MAS frequency of 4.0 kHz, and a  $^1\text{H}$  decoupling field of 70–80 kHz were used. Proton relaxation time values,  $^1\text{H } T_1$ , were measured *via* saturation recovery.

## RESULTS

### Solid-State NMR Spectroscopy of Gabapentin Forms

Figure 1 shows the  $^{13}\text{C}$  SSNMR spectrum of crystalline form II of gabapentin. The spectrum has one peak in the carbonyl region at 179 ppm and eight peaks in the aliphatic region between 20 and 60 ppm. The peak at 39 ppm is broadened due to coupling with  $^{14}\text{N}$ . This peak is useful for identifying different crystalline forms of gabapentin because

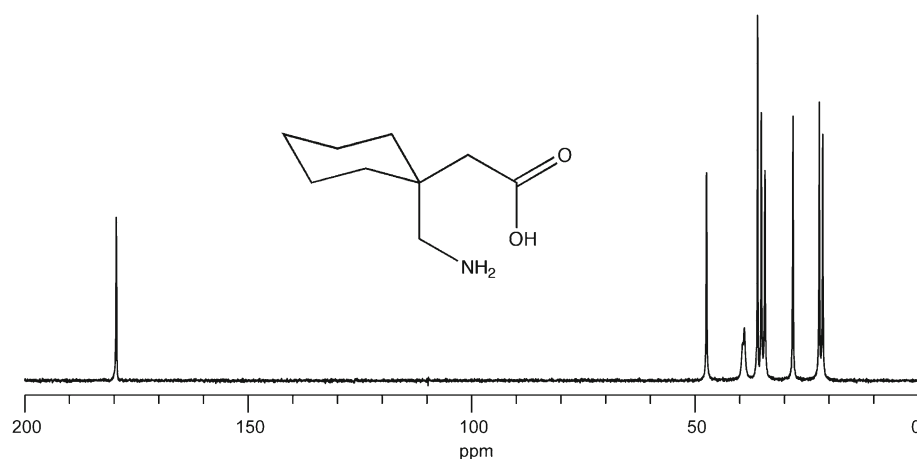


**Fig. 1.**  $^{13}\text{C}$  CP/MAS spectrum of gabapentin form II

of its distinctive lineshape. The linewidths of the other peaks vary from 10 to 15 Hz. The presence of nine peaks in the  $^{13}\text{C}$  SSNMR spectrum strongly suggests that there is only one crystallographically inequivalent molecule in the unit cell corresponding to nine carbon atoms in gabapentin, which is consistent with the single crystal XRD structure of form II (10).

Figure 2 shows the aliphatic region of the  $^{13}\text{C}$  SSNMR spectra of the different crystalline forms of gabapentin that have been analyzed in our laboratory, as well as gabapentin lactam. In addition to the SSNMR spectra of the forms reported in the literature, a SSNMR spectrum not

corresponding to any of those forms was observed during our characterization experiments. We attributed this spectrum to an additional form, which we refer to as the isomorphous desolvate (Fig. 2c). To the best of our knowledge, this form has not been reported in the literature. Although gabapentin form IV has been reported, we did not observe that form, and the PXRD of the new form was not consistent with that of form IV (8). In contrast to gabapentin form II, the crystalline forms I and III only have seven peaks in the aliphatic regions of the spectra. This is likely due to the overlapping peaks of two carbons between 20 and 25 ppm, which results in a broader peak at 22 ppm for form III and 22.5 ppm for form

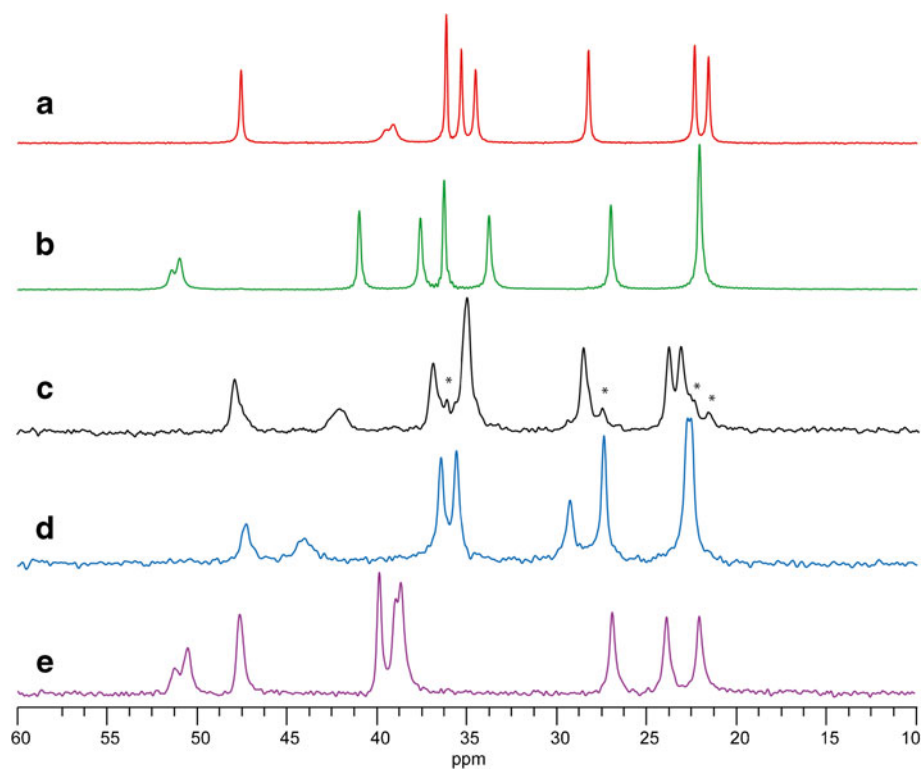


**Fig. 2.** Aliphatic region of  $^{13}\text{C}$  CP/MAS NMR spectra of solid forms of gabapentin and gabapentin lactam: **a** gabapentin form II; **b** gabapentin form III; **c** isomorphous desolvate; **d** gabapentin form I; **e** gabapentin lactam. The signal to noise of the spectra in **c–e** are poorer than the one of **a** and **b** because the  $^1\text{H}$   $T_1$  relaxation times of **c–e** are longer than that of **a** and **b**, and a smaller amount of acquisitions was used to collect them because of time constraints

**Table I.** Chemical Shifts of Carbon Peaks of Gabapentin Forms

	Chemical shifts (ppm)								
Form I	178.5	47.4	44.0	36.4	35.6	29.3	27.4	22.8	22.5
Form II	179.5	47.6	39.1	36.2	35.3	34.5	28.2	22.4	21.6
Form III	177.4	51.4	41.0	37.6	36.3	33.8	27.0	22.1	
Isomorphous desolvate	178.2	47.9	42.4	36.8	34.9	28.4	23.7	22.7	
Lactam	179.1	51.2	47.6	39.9	38.9	26.9	23.9	22.0	
		50.5			38.7				

The columns of the table do not reflect carbon assignments: the peaks are listed from the carbonyl peak to the last peak in the aliphatic region in the order that they appear in the spectrum

I. In form III, the carbon peak that is broadened due to  $^{14}\text{N}$  coupling is located at 51 ppm. There is a 12 ppm difference between the location of that peak in form II and form III. This large chemical shift difference is often seen in carbohydrates (17). The axial and equatorial position of the amine and carboxylic acid substituents are reversed when going from form II to form III.

The  $^{13}\text{C}$  SSNMR spectrum presented in Fig. 2c is a mixture of forms composed mainly of the isomorphous desolvate. Stars indicate the peaks that correspond to form I (22.8 and 27.4 ppm) and form II (21.6 and 36.2 ppm). The isomorphous desolvate was first encountered in the course of an NMR experiment: it was generated from the monohydrate upon loss of water through the hole in the endcap of the rotor. The  $^{13}\text{C}$  SSNMR spectrum of form I (Fig. 2d) has a different set of chemical shifts than observed for forms II and III.

Gabapentin lactam is the degradation product obtained from the dehydration of gabapentin to the cyclic lactam (Scheme 1). The aliphatic region of the gabapentin lactam  $^{13}\text{C}$  SSNMR spectrum has seven peaks. Two of these peaks (51 and 38 ppm) are broadened due to coupling with the adjacent  $^{14}\text{N}$  nucleus. The chemical shifts of the aliphatic carbons of gabapentin lactam are sufficiently different from those of the four crystalline forms of gabapentin to prevent confusion in form identification. Table I summarizes the  $^{13}\text{C}$

SSNMR chemical shifts of all the gabapentin forms analyzed as well as the gabapentin lactam.

In addition to differences in chemical shifts among the crystalline forms of gabapentin, there are also differences in proton spin-lattice relaxation time,  $^1\text{H}$   $T_1$ , values. SSNMR relaxation time values can be an indicator of the mobility of the sample, the amount of molecular disorder present, or particle size. Crystalline samples by definition possess long-range lattice order and may have long relaxation times. However, the presence of intrinsic relaxation sinks, such as a rotating methyl group, can lead to very short relaxation times. For example, ibuprofen and 3-methyl glutaric acid both have  $^1\text{H}$   $T_1$  values around 1 s (11,18). The  $^1\text{H}$   $T_1$  of as-received gabapentin form II is 134 s. This is a fairly long  $^1\text{H}$   $T_1$  and it indicates few defects in the crystal lattice and very low mobility. It also suggests that gabapentin form II is very stable, since defects facilitate chemical reactions to occur in the solid state. Gabapentin form III has a  $^1\text{H}$   $T_1$  value of 63 s. The  $^1\text{H}$   $T_1$  of gabapentin form I is 378 s. The presence of water within the crystal lattice likely explains the high magnitude of the  $^1\text{H}$   $T_1$  value. Water can act as a relaxation sink and cause shorter  $^1\text{H}$   $T_1$  times when it is mobile in the structure such as in non-stoichiometric hydrates or channel hydrates. However, when water is rigid in the crystal lattice, relaxation times can be longer.

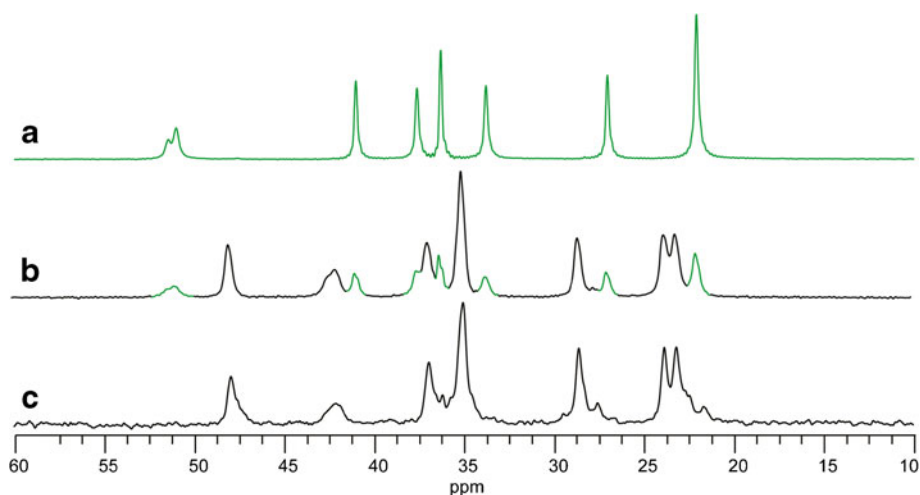


**Fig. 3.** Aliphatic region of  $^{13}\text{C}$  NMR spectra of **a** gabapentin form III, **b** spray-dried gabapentin, and **c** the isomorphous desolvate

**Table II.** Four Recrystallization Experimental Conditions and  $^1\text{H}$   $T_1$  and Lactam Levels Measured in Each Product

Lot	Recrystallization method	$^1\text{H}$ $T_1$ (s)	Lactam produced during thermal stress (% w/w)
A	Dissolved in 95% ethanol at 60°C, recrystallized at 60°C	63	0.174
B	Dissolved in anhydrous ethanol at 60°C, recrystallized at 60°C	128	0.019
C	Dissolved in 95% ethanol at 60°C, recrystallized at room temperature	110	0.112
D	Dissolved in anhydrous ethanol at 60°C, recrystallized at room temperature	131	0.003

The thermal stress conditions used were 50°C and 0% RH.  $^1\text{H}$   $T_1$  times are estimated to be within a 5% accuracy (24)

### Analysis of Mixtures

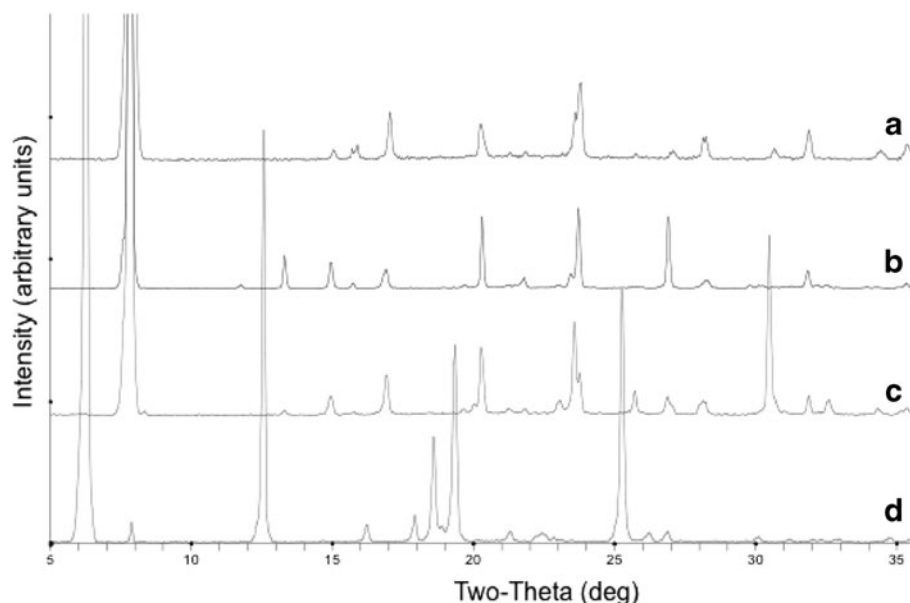
The aliphatic region of the spectra of form III, spray-dried gabapentin, and the isomorphous desolvate is shown in Fig. 3. The spectrum of spray-dried gabapentin (Fig. 3b) is a mixture of form III and the isomorphous desolvate. The ratio of form III to the isomorphous desolvate is approximately 75:25. The spray-dried gabapentin mixture showed two separate  $^1\text{H}$   $T_1$  values, which is consistent with it being a mixture of two different components. The peak at 51 ppm, identified to belong to form III, gave a  $^1\text{H}$   $T_1$  value of 17 s. The peak at 48 ppm belongs to the isomorphous desolvate and has a  $^1\text{H}$   $T_1$  of 39 s. It is unclear why the peaks of form III in the mixture are broader than the ones in the pure form III. One reason might be the susceptibility broadening of the spray-dried material. This effect was observed for ibuprofen where the linewidths were almost doubled when ibuprofen was crystallized from acetonitrile (18).

### Comparison of Analytical Techniques

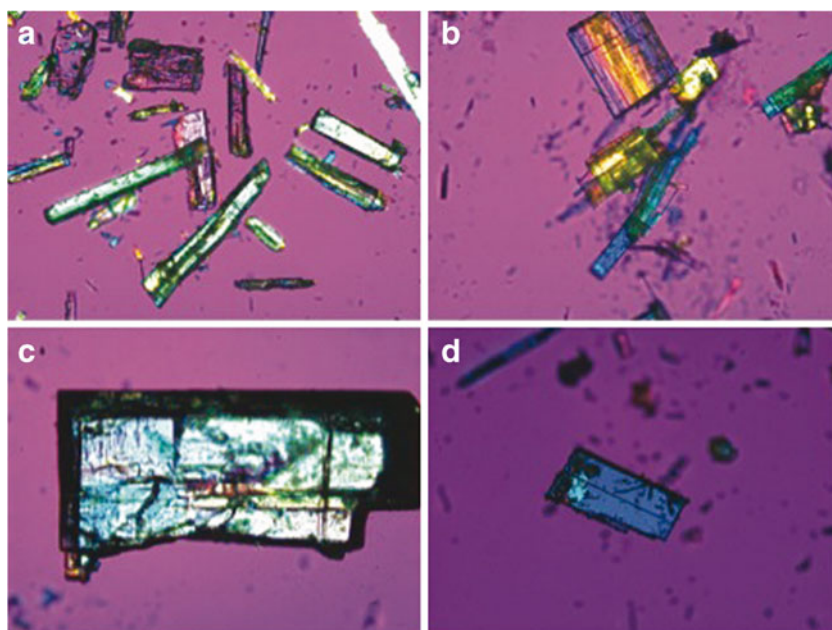
Four recrystallizations were performed using the conditions presented in Table II (hereafter referred to as lots A through D) and the products characterized by PXRD and SSNMR. The PXRD patterns of the four lots are shown in

Fig. 4. The intense peak at  $\sim 8^\circ 2\theta$  in the PXRD patterns of lots B, C, and D suggests that these three lots are mainly composed of form II. Nonetheless, there are differences in the locations and intensities of the weak peaks. Some of those differences can most likely be attributed to preferred orientation (19-22). Photomicrographs of lots A–D (Fig. 5) reveal that a large fraction of the crystals exhibits a pronounced habit (plates) and therefore preferred orientation is likely. A small peak at  $8.0^\circ 2\theta$  was observed in the pattern of lot A. Additionally, there are two intense peaks at  $6.0^\circ$  and  $12.5^\circ 2\theta$  that are absent in the patterns of the other three lots. All these observations suggest that lot A is a different form from lots B through D. In the absence of “reference standards,” PXRD was only of limited utility and did not permit definitive identification of the different forms. Since there were no pronounced halos in the PXRD patterns of the different lots (Fig. 4), we conclude that all the lots are substantially crystalline. Thus, differences in crystallinity could not explain the differences in chemical stability between the lots.

Figure 6 shows the aliphatic region of the  $^{13}\text{C}$  SSNMR spectra of the products of the four recrystallization experiments. Three of the recrystallization conditions, lots B through D, yielded form II, while one of them, lot A, generated form III. This identification can be made by comparing the chemical shifts of the carbons in the spectra



**Fig. 4.** PXRD patterns of the products of the four recrystallization experiments: **a** lot D; **b** lot C; **c** lot B; **d** lot A



**Fig. 5.** Polarized light microscopy images of representative samples of the products of the four recrystallizations: **a** lot A; **b** lot B; **c** lot C; **d** lot D

in Fig. 5 with those of the materials presented in Fig. 2, focusing on the chemical shift of the carbon peak split by  $^{14}\text{N}$  coupling. Lots B and C have comparable linewidths, ranging from 13 to 18 Hz. Lot D has the broadest peaks, with linewidths ranging from 22 to 28 Hz.

The recrystallization products were thermally stressed ( $50^\circ\text{C}/0\%$  relative humidity (RH)), and the amount of gabapentin lactam generated was calculated by subtracting the amount of lactam

present in each sample before thermal stress from that after the thermal stress (Table II). The table also contains the  $^1\text{H}$   $T_1$  values of the four recrystallized lots. Lot A has the shortest relaxation time value, 63 s, and was most affected by the thermal stress (0.174% lactam). Lots B and D have the longest relaxation time values, 128 and 131 s, respectively, and they generated the least amount of lactam—0.019% in lot B and 0.003% in lot D. This may be a coincidence because there is not necessarily a direct

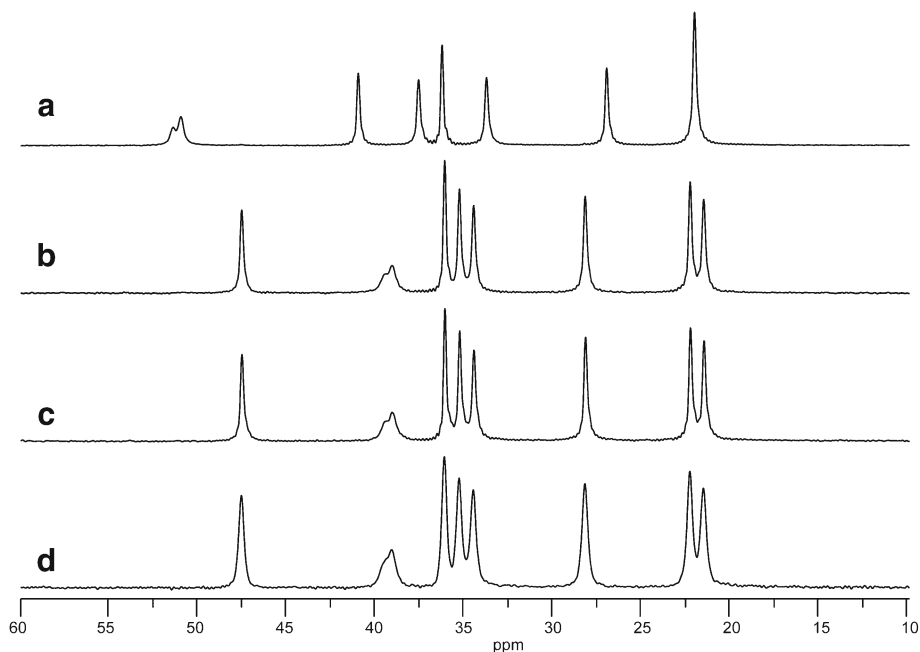


**Fig. 6.** Aliphatic region of  $^{13}\text{C}$  CP/MAS spectra of products of the four recrystallization experiments: **a** lot A; **b** lot B; **c** lot C; **d** lot D. See Table II for details on preparation of the lots

**Table III.** Milling Conditions and Measured  $^1\text{H}$   $T_1$  Values and Lactam Levels for Each Sample

Milling conditions	$^1\text{H}$ $T_1$ (s)	$\Delta$ lactam
Gabapentin form II	134	0.000
Gabapentin form II milled for 45 min	41	0.109
Gabapentin form II milled for 45 min and exposed to 50°C/0% RH for 24 h	61	0.134
Gabapentin form II–HPC (6.5%) mixture	130	0.011
Gabapentin form II–HPC (6.5%) mixture milled for 45 min	11	0.464
Gabapentin form II–HPC (6.5%) milled for 45 min and exposed to 50°C/0% RH for 24 h	14	0.467

correlation between the relaxation times of different polymorphs and their relative stability.

Polarized light microscopy images of the recrystallized lots, presented in Fig. 5, show that there are differences in morphology. Lots B, C, and D are plate-like crystals, whereas lot A is mostly composed of needles. The plate morphology of lots B, C, and D could explain the line broadening observed in their SSNMR spectra. Under polarized light, single crystals appear yellow or blue depending on the rotation of the stage, and agglomerates composed of single crystals appear green. Lots B and D are mostly single crystals, while lot C is not (23). This is consistent with lots B and D having longer  $^1\text{H}$   $T_1$  values than lot C.

#### Effect of Milling and HPC on Form Conversion and Lactam Formation

As-received gabapentin form II was milled for 45 min and then stored or exposed to 50°C/0% RH. All the samples were then thermally stressed (50°C/0% RH) following this

treatment. The same experimental process was used for gabapentin form II mixed with 6.5% (*w/v*) HPC. The lactam content was measured before and after thermal stress. Table III summarizes the results. Based on the lactam levels present in the samples after thermal stress, three categories emerge: low, medium, and high stability. The high stability group contained less than 0.01% of lactam. It includes as-received gabapentin form II and gabapentin form II mixed with 6.5% HPC. The medium stability group contained between 0.01% and 0.1% of lactam, and the low stability group contained more than 0.4% lactam.

Figure 7a, b shows the aliphatic region of the  $^{13}\text{C}$  SSNMR spectra of as-received gabapentin form II and gabapentin form II mixed with 6.5% HPC, respectively. The spectra of these two samples display the same carbon chemical shifts and similar linewidths of approximately 12–14 Hz. This indicates that the HPC mixed with as-received gabapentin form II in a physical mixture has no effect on the physical form of gabapentin. Subpanels c and d of Fig. 7, respectively, show

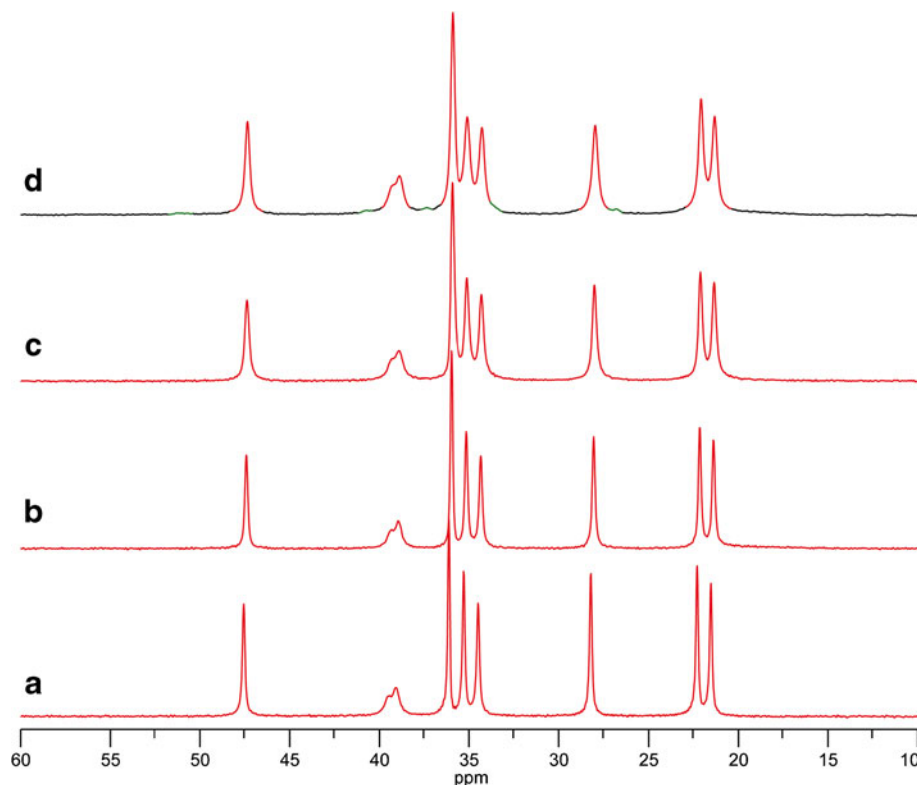


**Fig. 7.** Aliphatic region of  $^{13}\text{C}$  CP/MAS spectra of **a** gabapentin form II; **b** gabapentin form II mixed with 6.5% (*w/v*) HPC; **c** gabapentin form II milled for 45 min; **d** gabapentin form II mixed with 6.5% HPC and milled for 45 min

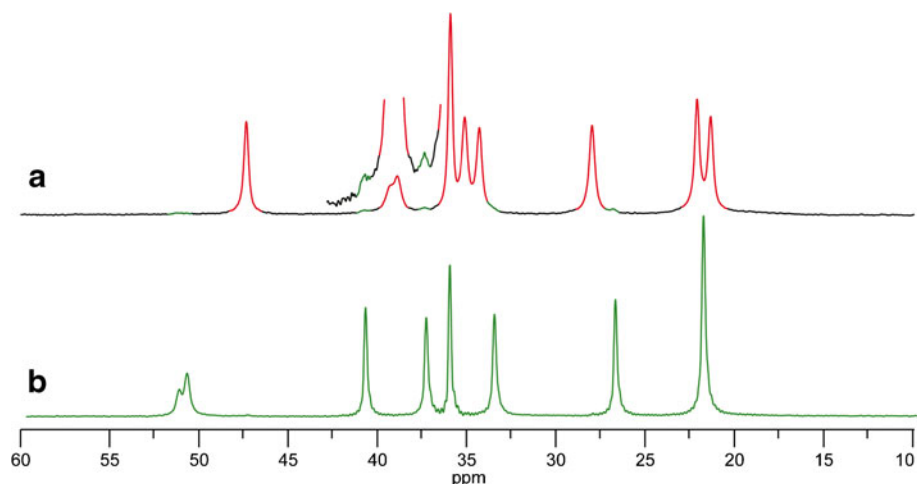


**Fig. 8.** Aliphatic region of  $^{13}\text{C}$  CP/MAS spectra of **a** gabapentin form II mixed with 6.5% (*w/v*) HPC and milled for 45 min; **b** gabapentin form III

the aliphatic regions of the  $^{13}\text{C}$  SSNMR spectra of milled gabapentin form II and of gabapentin form II mixed with 6.5% HPC and milled. The two spectra have eight peaks with chemical shifts corresponding to gabapentin form II. The spectrum in Fig. 7d presents small peaks at 37 and 41 ppm. Gabapentin milled alone shows no such peaks. Figure 8 shows that these small peaks align with two of the peaks of form III. Therefore, when milled in the presence of HPC (6.5% *w/v*), a small fraction of gabapentin form II converted to form III. Other groups have also reported gabapentin form conversion in the presence of a variety of excipients (5,6).

Figure 9a shows the aliphatic region of the  $^{13}\text{C}$  SSNMR spectrum of the unmilled physical mixture of gabapentin form II and HPC. Figure 9b, c shows spectra of the milled gabapentin–

HPC physical mixture. All three spectra have similar chemical shifts, which correspond to form II. Both gabapentin co-mixed with 6.5% HPC and gabapentin co-mixed with 6.5% HPC, milled and exposed to 50°C and 0% relative humidity, contain a small amount of form III as evidenced by two small peaks at 37 and 41 ppm. There are very obvious differences in linewidths among the samples. The milled samples have broader linewidths (20 Hz) than the unmilled samples (12 Hz) suggesting that the former are less homogeneous than the latter.

There are significant differences in  $^1\text{H}$   $T_1$  values between the milled and unmilled gabapentin and gabapentin–HPC samples. Gabapentin and gabapentin–HPC mixture have the same  $^1\text{H}$   $T_1$  value of ~130 s. This suggests that they both have similar mobility and similar physical stability. This is not

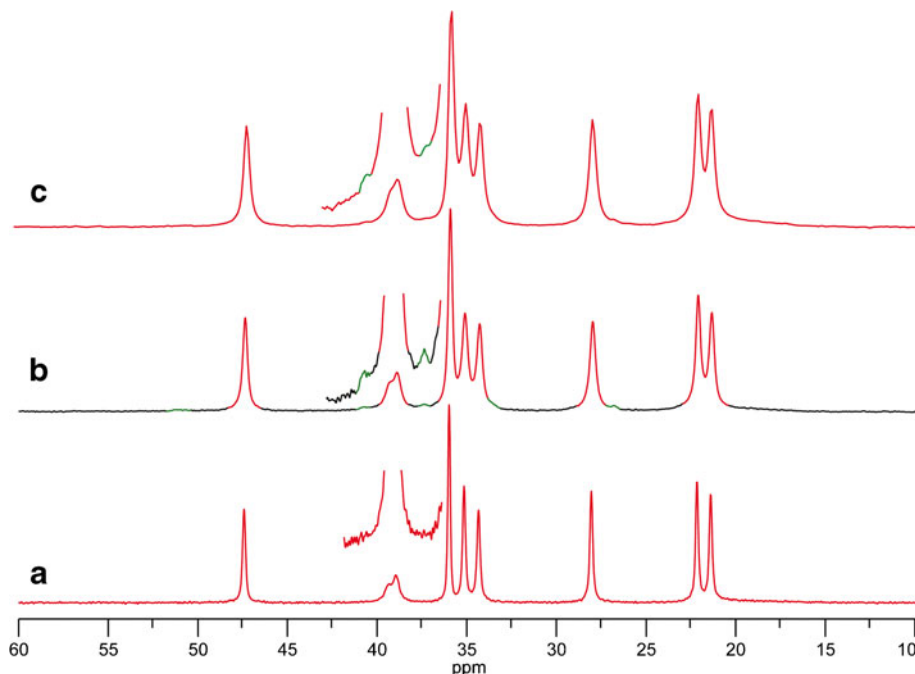


**Fig. 9.** Aliphatic region of  $^{13}\text{C}$  CP/MAS spectra of **a** gabapentin form II mixed with 6.5% (*w/v*) HPC; **b** gabapentin form II mixed with 6.5% (*w/v*) HPC and milled for 45 min; **c** gabapentin form II mixed with 6.5% (*w/v*) HPC, milled for 45 min and exposed to 50°C and 0% RH. A blow-up of the spectral region containing peaks of form III is presented above each spectrum



surprising because of the small amount of HPC present and the fact that this sample was prepared as a physical mixture. The  $^1\text{H}$   $T_1$  of gabapentin milled alone varied from 41 to 61 s depending on the post-milling conditions. The two gabapentin-HPC milled samples have significantly lower  $^1\text{H}$   $T_1$  values than gabapentin form II: 11 and 14 s. Both samples generated  $\sim 0.5\%$  of lactam during thermal stress. These two samples also generated a detectable amount of gabapentin form III upon milling.

## DISCUSSION

The milled gabapentin form II had a  $^1\text{H}$   $T_1$  value an order of magnitude shorter than the unmilled material. A similar trend was observed in work performed in our laboratory on lactose monohydrate cryoground for various lengths of time (9). Cryogrinding the as-received material for only 2 min reduced the  $^1\text{H}$   $T_1$  value by more than 200 s. Lactose monohydrate cryoground for 60 min had a  $^1\text{H}$   $T_1$  value two orders of magnitude shorter than the as-received material. As-received lactose monohydrate is crystalline. However, increasing cryogrinding times lead to increased level of amorphous material in the sample. Only a small amount of crystalline material was observed in the SSNMR spectrum of the lactose cryoground for 60 min. It was hypothesized that the amorphous material acted as a relaxation sink, leading to shorter relaxation times. In the case of gabapentin, milling did not generate any amorphous material, although peak broadening did occur. The changes in relaxation time were probably due to particle size reduction, as well as creation of crystal defects. It is possible that these smaller particles and crystal defects act similarly to the amorphous material in lactose monohydrate, causing the decrease in relaxation time observed. The observed line broadening of the milled samples could be explained by susceptibility broadening due to induced anisotropic bulk magnetic susceptibility.

The magnitude of the relaxation time of the gabapentin samples is correlated to the amount of crystal defects present: the more defects present, the shorter the relaxation time. Since defects are typically the sites where solid-state reactions take place, the relaxation time is then indirectly correlated to the stability of the material. Milled gabapentin samples with the shortest relaxation times produced the largest amounts of lactam.

Gabapentin form II when milled in the presence of HPC converted to the metastable form III. This did not occur in the absence of HPC. In addition, a significantly larger amount of lactam was generated in the milled gabapentin form II-HPC samples than in the gabapentin samples milled alone. These samples also had shorter  $^1\text{H}$   $T_1$  values than the other milled material. These two observations indicate that milling gabapentin in the presence of HPC creates material that is less stable than the gabapentin milled alone.

## CONCLUSION

Gabapentin polymorphic forms could be identified based on differences in SSNMR chemical shifts. In addition, we identified a new form of gabapentin, denoted as the isomorphous desolvate. Furthermore, we have established that differences in relaxation time values can provide us with some

information on the relative stability of the samples. Samples with shorter  $^1\text{H}$   $T_1$  values generated a greater amount of gabapentin lactam when placed under thermal stress, than samples with longer  $^1\text{H}$   $T_1$  values. This suggests that a decrease in gabapentin relaxation time can be correlated with reduced chemical stability.

## ACKNOWLEDGMENTS

We are grateful to the National Institute for Pharmaceutical Technology and Education and the U.S. Food and Drug Administration (FDA) for providing funds for this research. This study was funded by the FDA-sponsored contract #HHSF223200819929C "Development of Quality by Design (QbD) Guidance Elements on Design Specifications Across Scales with Stability Considerations."

EJM is a partial owner of Kansas Analytical Services, a company that provides solid-state NMR services to the pharmaceutical industry. The results presented here are from EJM's academic work at the University of Kansas and the University of Kentucky, and no data from Kansas Analytical Services is presented here.

## REFERENCES

1. Reece HA, Levendis DC. Polymorphs of gabapentin. *Acta Crystallogr C*. 2008;64(3):o105–8.
2. Hsu CH, Ke WT, Lin SY. Progressive steps of polymorphic transformation of gabapentin polymorphs studied by hot-stage FTIR microspectroscopy. *J Pharm Pharm Sci*. 2010;13(1).
3. Wenger M, Bernstein J. An alternate crystal form of gabapentin: a cocrystal with oxalic acid. *Cryst Growth Des*. 2008;8(5):1595–8.
4. Reddy LS, Bethune SJ, Kampf JW, Rodriguez-Hornedo N. Cocrystals and salts of gabapentin: pH dependent cocrystal stability and solubility. *Cryst Growth Des*. 2008;9(1):378–85.
5. Lin S-Y, Hsu C-H, Ke W-T. Solid-state transformation of different gabapentin polymorphs upon milling and co-milling. *Int J Pharm*. 2010;396(1–2):83–90.
6. Cutrignelli A, Denora N, Lopedota A, Trapani A, Laquintana V, Latrofa A, *et al*. Comparative effects of some hydrophilic excipients on the rate of gabapentin and baclofen lactamization in lyophilized formulations. *Int J Pharm*. 2007;332(1):98–106.
7. Zong Z, Desai SD, Kaushal AM, Barich DH, Huang H-S, Munson EJ, *et al*. The stabilizing effect of moisture on the solid-state degradation of gabapentin. *AAPS PharmSciTech*. 2011;12:924–31. doi:10.1208/s12249-011-9652-8.
8. Braga D, Grepioni F, Maini L, Rubini K, Polito M, Brescello R, *et al*. Polymorphic gabapentin: thermal behaviour, reactivity and interconversion of forms in solution and solid-state. *New J Chem*. 2008;32(10):1788–95.
9. Lubach JW, Xu D, Segmuller BE, Munson EJ. Investigation of the effects of pharmaceutical processing upon solid-state NMR relaxation times and implications to solid-state formulation stability. *J Pharm Sci*. 2007;96(4):777–87.
10. Ibers JA. Gabapentin and gabapentin monohydrate. *Acta Crystallogr C*. 2001;57(5):641–3.
11. Barich DH, Gorman EM, Zell MT, Munson EJ. 3-Methylglutaric acid as a  $^{13}\text{C}$  solid-state NMR standard. *Solid State Nucl Magn Reson*. 2006;30(3–4):125–9.
12. Pines A, Gibby MG, Waugh JS. Proton-enhanced nuclear induction spectroscopy  $^{13}\text{C}$  chemical shielding anisotropy in some organic solids. *Chem Phys Lett*. 1972;15(3):373–6.
13. Pines A. Proton-enhanced NMR of dilute spins in solids. *J Chem Phys*. 1973;59(2):569. doi:10.1063/1.1680061.
14. Andrew ER, Bradbury A, Eades RG. Removal of dipolar broadening of nuclear magnetic resonance spectra of solids by specimen rotation. *Nature*. 1959;183(4678):1802–3. doi:10.1038/1831802a0.

15. Dixon WT, Schaefer J, Sefcik MD, Stejskal EO, McKay RA. Total suppression of sidebands in CPMAS C-13 NMR. *J Magn Reson.* 1982;49(2):341–5. 1969.
16. Fung BM, Khitrin AK, Ermolaev K. An improved broadband decoupling sequence for liquid crystals and solids. *J Magn Reson.* 2000;142(1):97–101.
17. Chen Y-Y, Luo S-Y, Hung S-C, Chan SI, Tzou D-LM. <sup>13</sup>C Solid-state NMR chemical shift anisotropy analysis of the anomeric carbon in carbohydrates. *Carbohydr Res.* 2005;340(4):723–9.
18. Barich DH, Davis JM, Schieber LJ, Zell MT, Munson EJ. Investigation of solid-state NMR line widths of ibuprofen in drug formulations. *J Pharm Sci.* 2006;95(7):1586–94.
19. Stephenson GA, Forbes RA, Reutzel-Edens SM. Characterization of the solid state: quantitative issues. *Adv Drug Deliv Rev.* 2001;48(1):67–90.
20. Hurst VJ, Schroeder PA, Styron RW. Accurate quantification of quartz and other phases by powder X-ray diffractometry. *Anal Chim Acta.* 1997;337(3):233–52.
21. Campbell Roberts SN, Williams AC, Grimsey IM, Booth SW. Quantitative analysis of mannitol polymorphs. X-ray powder diffractometry, exploring preferred orientation effects. *J Pharm Biomed Anal.* 2002;28(6):1149–59.
22. Anwar J, Tarling SE, Barnes P. Polymorphism of sulfathiazole. *J Pharm Sci.* 1989;78(4):337–42.
23. Brunsteiner M, Jones AG, Pratola F, Price SL, Simons SJR. Toward a molecular understanding of crystal agglomeration. *Cryst Growth Des.* 2005;5(1):3–16. 2004.
24. Gorman EM. Solid-state physical form detection and quantitation of pharmaceuticals in formulations [3449658]. PhD Dissertation Lawrence: University of Kansas; 2011.